Available online at www.sciencedirect.com
SCIENCE DIRECT
Journal of Catalysis 235 (2005) 359–367
JOURNAL OF CATALYSIS
www.elsevier.com/locate/jcat

Reactivity of oxidized copper surfaces in methanol oxidation

L. Zhou [a], S. Günther [b], D. Moszynski [c], R. Imbihl [a,*]

[a] *Institut für Physikalische Chemie und Elektrochemie, Universität Hannover, Callinstrasse 3-3a, D-30167 Hannover, Germany*
[b] *Department Chemie, Ludwig-Maximilians-Universität München, Butenandstrasse 11 E, D-81377 München, Germany*
[c] *Technical University of Szczecin, Institute of Chemical and Environment Engineering, ul. Pulaskiego 10, 70-322 Szczecin, Poland*

Received 12 May 2005; revised 23 August 2005; accepted 23 August 2005

Abstract

The reactivity of metallic and oxidized copper surfaces in methanol oxidation was studied in the 10^{-2} mbar range. Transitions between the metallic surface and the two copper oxides, Cu_2O and CuO, are being followed by the color changes of the sample and by ellipsometric measurements. Compared with a metallic copper surface, a partially oxidized copper surface has higher reactivity toward production of formaldehyde, whereas the deeply oxidized surface (CuO) shows a higher activity toward total oxidation to CO_2. Oxidation and reduction of the Cu surface are associated with a strong change in the degree of roughening and with spatial inhomogeneities, as demonstrated by photographic imaging and by ellipsometric microscopy.

Keywords: Methanol oxidation; Copper; Copper oxide; Formaldehyde; Surface reactivity; Partial oxidation; Ellipsometry

1. Introduction

The mechanism of methanol oxidation on copper surfaces has been studied extensively because of its relevance to the industrially important catalytic synthesis of formaldehyde [1,2]. Although in industrial processes silver is still used mainly for the partial oxidation of methanol to formaldehyde, high yields have been obtained with copper catalysts under ultrahigh-vacuum (UHV) conditions. In addition, the interaction of methanol with copper surfaces is a key mechanistic step in several technologically important catalytic processes, including methanol synthesis from "syngas" over Cu/ZnO catalysts and methanol steam reforming over Al_2O_3-supported Cu/ZnO [3–7].

Numerous high-pressure studies [8–16] and low-pressure single-crystal investigations [17–37] have been published in the past two decades focusing on various aspects of this reaction system. In particular, identifying the active surface phases and the relevant surface species has been the aim of various in situ studies.

Single-crystal investigations have focused on the Cu(110) surface, applying temperature-programmed desorption (TPD), molecular beam techniques, and scanning tunnelling microscopy (STM) [17–26]. It has been shown that both the oxygen-free surface and a surface fully covered with (2×1)-O islands (0.5 ML oxygen coverage) have very low reactivity for the dissociative adsorption of methanol. In contrast, a surface partially covered with (2×1)-O islands (about 0.25 ML oxygen coverage) exhibits a pronounced maximum in oxidation activity. A reaction mechanism with methoxy and formate species as intermediates has been suggested [17–26]. In recent high-pressure studies ($p \leqslant 10$ mbar) with polycrystalline copper samples, a novel suboxide species was detected using in situ X-ray absorption spectroscopy (XAS) and X-ray photoelectron spectroscopy (XPS) [9–14,16]. This new oxygen species, which exists only under reaction conditions at high pressure, was found to be correlated with a high yield of formaldehyde. Besides defining the active state of the catalyst, the reaction system also displayed interesting dynamic behavior. Rate oscillations associated with complex temporal variations of different reaction products were discovered at pressures $>10^{-2}$ mbar.

* Corresponding author. Fax: +49 511 762 4009.
E-mail address: imbihl@pci.uni-hannover.de (R. Imbihl).

0021-9517/$ – see front matter
doi:10.1016/j.jcat.2005.08.020

These oscillations were connected with periodic transitions of the sample surface between metallic copper and copper oxides [8,15].

In this paper we compare the reactivities of metallic and oxidized copper surfaces in methanol oxidation in the 10^{-2} mbar range. During methanol oxidation, transitions of the catalytic surface between deeply oxidized copper CuO, Cu_2O, and metallic copper were observed visually and by ellipsometry as in situ technique. Besides the conventional use in monitoring layer growth, ellipsometry applied as microscopy can also be used to detect spatial inhomogeneities in the oxidation and reduction of copper surfaces.

2. Experimental

All experiments were carried out in a high-pressure reaction cell with a volume of about 0.1 L and a pumping rate of about 0.4 L/s (Fig. 1). This cell was connected to an UHV chamber with a sample transfer system of about 8 L volume. Rate measurements were performed with a differentially pumped quadrupole mass spectrometer (QMS, Hiden HALO201). Because the reaction cell could not be closed gas-tight against the 8-L volume of the transfer system, we cannot give absolute numbers for the reaction rates but can give only the relative rate; that is, we compare the reactivity. The high-pressure reaction cell had been designed for the in situ application of a commercial ellipsometer (Optrel Multiskop). Two quartz windows for the ingoing and outgoing laser beam were used, giving a reflection angle of 70° with respect to the surface normal.

In integrative ellipsometric measurements, the two angles characterizing the change in polarization, Δ and Ψ, were determined in a so-called "1/3-zone" scheme measuring the reflected light intensity over a 1×2 mm^2 illuminated sample area using a photodiode as a detector. In the imaging mode of ellipsometry, a lens and a 1/2-inch monochromatic CCD camera instead of the detector provides surface images with ellipsometric contrast.

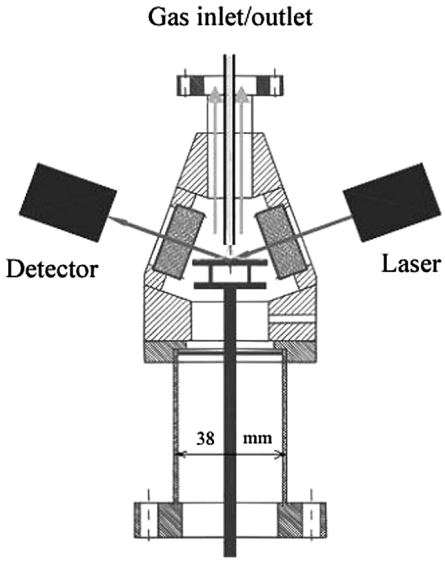

Fig. 1. Schematic drawing of the high pressure reaction cell for in situ ellipsometry.

A Cu(110) single crystal (1.5 mm thick, 9×11 mm^2), was used as catalyst. The originally flat and atomically well-ordered surface that had been used in previous UHV experiments was roughened considerably during the experiments at high pressure, changing to a polycrystalline structure. The sample was firmly mounted on an SiC-coated BN button heater (Sintec) enabling temperature-programmed experiments in the 298–750 K range.

Linear heating ramps were adjusted using a PID controller (Eurotherm 2416), connected to a programmable power supply (DELTA ES030-10) that feed the button heater. The sample temperature was monitored by a chromel-alumel thermocouple attached to the edge of the sample.

All gases were introduced via mass flow controllers (MKS 1179) and reached the sample surface through a 3-mm i.d. stainless steel tube that faced the sample at a distance ≈2 mm normal to the sample surface. The gases impinged on the central part of the sample flowing away in radial direction, thus establishing a circular symmetry. At 10^{-2} mbar, the mean free path of gases at 300 K is in the range of a few centimeters, meaning that all molecules leaving the tube opening will impinge on the surface. The gases were pumped out of the reactor through an exhaust concentrically mounted around the gas inlet pipe (Fig. 1) and then through an adjustable needle valve (Pfeiffer EVN116) to the turbo molecular pump (60 L/s). Gas flows of 0.1–0.3 sccm were adjusted. The pressure in the reaction cell was measured by a Baratron pressure gauge (MKS 622A).

Calibration gases (H_2, H_2O, CO, formaldehyde, methanol, O_2, and CO_2) were applied to relate the QMS signal to partial pressures in the reaction cell. For water and methanol, the vapor pressure over the liquid phase proved sufficient, and for formaldehyde, the vapor pressure of solid para-formaldehyde was used. Oxygen of purity 5.0 (99.999%) and methanol of purity 2.8 (99.8%) served as reactants. From background-corrected intensities of the detected masses ($m/e = 2$, 18, 28, 30, 31, 32, 44) and the total pressure in the reaction cell, the true partial pressures were calculated by a matrix inversion technique, which takes the fragmentation pattern of the different molecules into account. From the absolute partial pressures, the H-, O-, and C-mass balance could be checked for all TPR spectra presented here. Mass conservation for carbon, checked by comparing the total consumption and total production for all C-containing molecules, is >5%.

3. Results

3.1. Reaction kinetics

Kinetic measurements were carried out over three differently prepared Cu(110) sample surfaces: (a) a metallic surface obtained after the sample had been completely reduced by methanol, yielding a yellow shining surface; (b) a partially oxidized surface after the sample had been exposed to oxygen (1 mbar, 423 K, 5 min) until a red sample with a Cu_2O film was formed; and (c) a deeply oxidized surface when the sample

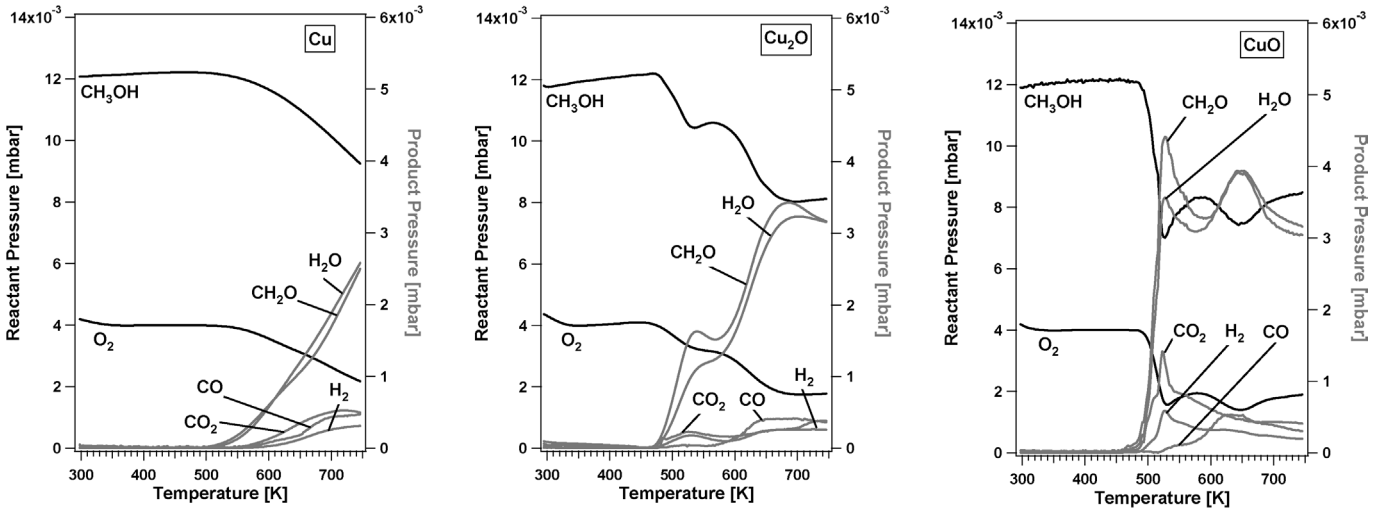

Fig. 2. Temperature programmed reaction spectra in the 10^{-2} mbar range over three different sample surfaces: metallic copper surface (left), a partially oxidized copper red surface with a Cu_2O film (middle), and a deeply oxidized black copper surface with a CuO film (right). Shown is the heating part of the experiment with a heating rate of 5 K/min. A CH_3OH flow rate of 0.3 sccm (standard cubic centimeter per minute) and an O_2 flow rate of 0.1 sccm were applied.

had been oxidized by oxygen (1 mbar, 673 K, 30 min) until a black CuO film was observed. Both oxidation processes caused visible roughening of the initially flat Cu surface.

Fig. 2 compares the TPR spectra of the three surfaces obtained with a linear heating rate as slow as 5 K/min under identical conditions. A methanol to oxygen mixing rate of 3:1 was chosen, with an oxygen flow of 0.1 sccm.

On the metallic copper surface, the reaction ignited at ≈500 K, and the surface reactivity slowly increased with increasing temperature. Methanol conversion reached a maximum of ≈25% at 750 K. Formaldehyde was always the dominant product, whereas the contribution of the total oxidation product, CO_2, remained moderate even at elevated temperatures. In low-pressure UHV studies, methanol oxidation on a Cu(110) surface exhibited two rate maxima, one at ≈400–520 K and another at 900 K [38,39]. The reactive sticking coefficient for methanol reached as high as ≈0.25 for Cu(110)/$CH_3OH + O_2$ [38,39]. The amplitude of the low-temperature reactivity peak decreased with increasing total pressure, vanishing beyond 10^{-3} mbar. This low-T reactivity peak thus should not exist at higher pressure, in agreement with the results in Fig. 2. Recent in situ XPS of methanol oxidation over Cu(110) in the 0.1 mbar range showed that at low temperatures the copper surface was covered by methoxy, adsorbed oxygen, and formate species, which block the surface [13,14]. Higher temperatures were required to slowly activate the surface.

Compared with the metallic copper surface, both oxidized surfaces showed higher reactivity. The kinetics exhibited two rate maxima, as illustrated in Fig. 2. On the Cu_2O surface, the reaction already started at 480 K. After passing a relative maximum at 530 K, the reactivity increased further, reaching a second reactivity peak at ≈700 K. The deeply oxidized surface exhibited the highest reactivity and an even lower initial reaction temperature (≈450 K). With higher reactivity, the partially oxidized surface maintained the fairly high selectivity to formaldehyde. Compared with the Cu_2O surface, the deeply oxidized CuO sample showed more total oxidation to CO_2, although formaldehyde was still the predominant product.

It should be pointed out that the reaction was only on the metallic copper surface in a steady state, whereas the reaction rates of the oxidized surfaces were all nonstationary; that is, the reaction rate changed with time under constant reaction conditions. In separate experiments, when the heating ramp was stopped at 520 and 650 K, these surfaces slowly changed color and morphology, accompanied by a time-dependent variation of the reaction rate. Apparently, a reduction occurred involving not only the surface oxygen, but also the bulk oxygen. The time scale of this process is on the order of 1 to several minutes.

The color and roughness changes associated with the formation of different Cu oxides make it easy to follow the surface changes in the TPR experiments with optical microscopy. Fig. 3 shows a set of photographic images of the sample in the reactor during a TPR, starting from a deeply oxidized copper sample. The images were taken with a digital camera with a fixed aperture and white balance, so that the true sample color was recorded. The related TPR spectrum is also shown in the figure. The arrows at the top part of the panel indicate the reactivity corresponding to each displayed image. Here, the mixing ratio of methanol to oxygen was 2:1 and the oxygen flow rate was 0.1 sccm.

At the beginning of the reaction, the deeply oxidized sample exhibited a very rough black surface indicative of CuO. Only after ignition of the reaction at $T \approx 510$ K did the surface start to change notably. Starting from the center of the sample, the copper(II) oxide was converted to the red Cu_2O oxide associated with a flattening of the surface roughness on a ⩾100-μm scale. As judged from the images, this process was completed around 650 K. At this temperature, the reactivity exhibited a pronounced relative maximum only slightly below the first reactivity peak located immediately after ignition of the reaction. Above 650 K, the slow change of the surface to a yellow shining state indicates reduction of the copper(I) oxide to a metallic surface. During several stages of the reaction, the sample was

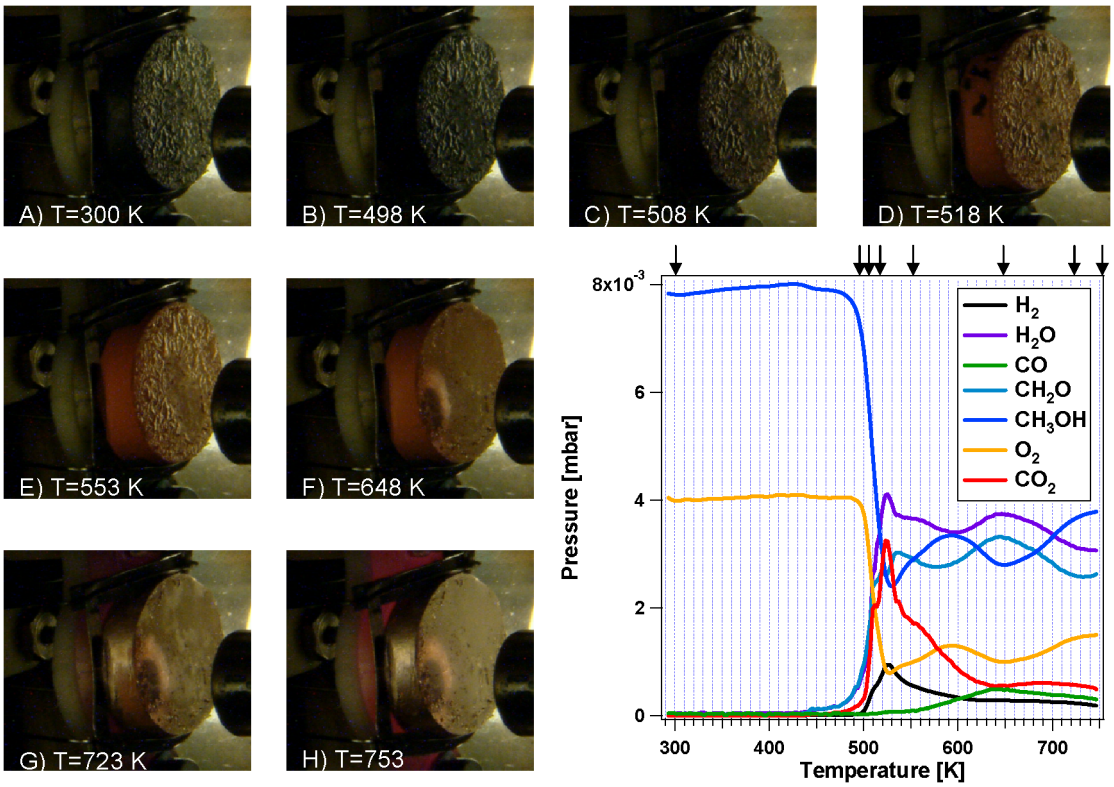

Fig. 3. Photographic images showing changes of the oxide phase during a TPR experiment over a deeply oxidized copper. Shown is the heating part of the experiment with a heating rate of 5 K/min. The TPR spectra are included with arrows indicating where the corresponding photographic images were taken. Reaction conditions: CH_3OH flow rate 0.2 sccm and O_2 flow rate 0.1 sccm.

completely opaque, indicative of extensive light scattering due to a high amount of surface roughness on a $\leqslant$1-μm scale.

Note that under nearly all conditions, formaldehyde is the preferred reaction product. Only directly after ignition on the CuO surface and for a short time was the total oxidation product CO_2 of higher intensity than formaldehyde. With progressive reduction of the surface, the CO_2 channel decayed rapidly in intensity, finally approaching the low level characteristic of a metallic surface. The foregoing data show a more or less complete reduction of the deeply oxidized copper sample associated with a drastic change in surface morphology. To obtain more information about the thickness of the oxide layers, we applied ellipsometry as in situ technique to study the surface chemistry of the sample during the TPR experiments.

3.2. Ellipsometric measurements

Ellipsometry is a well-established technique for characterizing thin films and surfaces that allows the determination of optical constants and thickness of layer systems [40]. Ellipsometry uses the fact that the state of polarization of an incident photon beam changes in reflection at a surface. The change in the state of polarization can be described by two angles, Δ and Ψ, obtained in a so-called "null-setting" experiment, which in turn are related to the optical properties of the film. From the measured Δ and Ψ values, the thickness of the surface layers can be extracted for a multilayer surface model, provided that the chemical identity of the different layers has been determined and the optical constants for these layers are known. The information depth of the ellipsometric measurement for a given geometry is limited by the penetration depth of light in the solid material. In our case with a wavelength of ≈630 nm, a depth of 0.1–6 μm was obtained, with the small value referring to metallic Cu and the large value belonging to Cu_2O.

Fig. 4 shows Δ and Ψ variation measured in situ during a TPR experiment on a deeply oxidized copper surface. The corresponding TPR spectrum is included in the same diagram. The variation in Δ and Ψ reflects the slow conversion from a CuO surface to Cu_2O and finally to a metallic Cu surface.

For simulating the measured Δ and Ψ values, a realistic sequence of model layers had to be found that explains the observed variation of Δ and Ψ in a consistent way. In all simulations the incident beam angle was set to 70°; the optical constants for the gas phase, which must be included, were chosen as $n = 1$ (refractive index) and $k = 0$ (extinction coefficient); whereas for the different Cu and Cu oxide phases of the sample, the values for n, k, and the resulting Brewster angle, φ_p, at the light wavelength of $\lambda = 6328$ Å are listed in Table 1 [41].

With more than one layer involved, no unique fit exists for a measured single pair of Δ and Ψ angles. However, we found only one layer sequence over which the entire temperature range could be fitted and that does not contradict chemical intuition and the literature data. The resulting sequence was as follows. The initial deeply oxidized copper sample was modeled by a layer of copper(II) oxide on top of metallic bulk Cu (i.e., CuO/Cu bulk). At temperatures above 480 K, the sam-

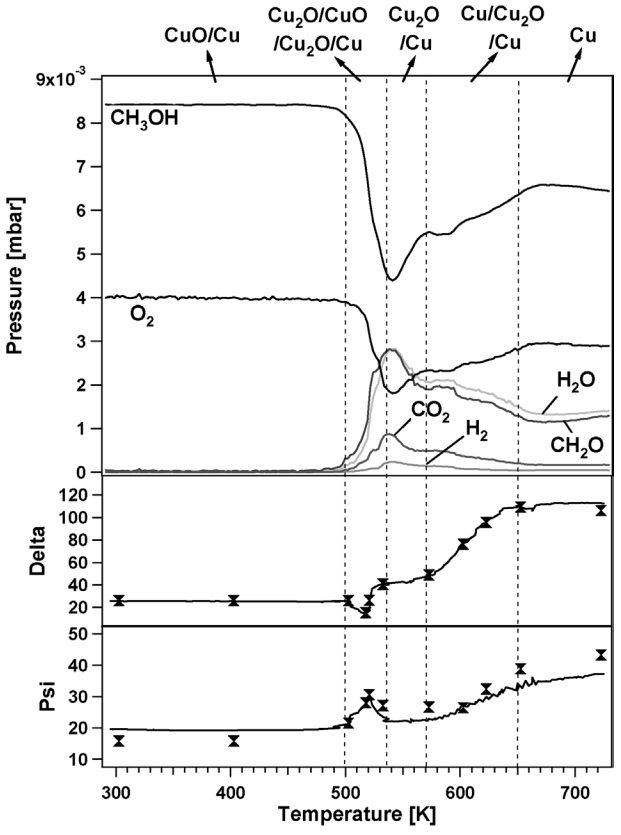

Fig. 4. Reaction rates combined with ellipsometric measurements showing the variation of Δ and Ψ values during a TPR experiment over a deeply oxidized copper sample. Shown is the heating part of the experiment with a heating rate of 5 K/min. The Δ and Ψ values simulated with a layer model are represented as triangular markers. Vertical lines separate different layer sequences (see text). Reaction conditions: CH_3OH flow rate 0.2 sccm and O_2 flow rate 0.1 sccm.

ple was partially reduced, resulting in a more complicated sequence. Between 490 and 520 K, coexisting oxides with a sequence $Cu_2O/CuO/Cu_2O/Cu$ bulk were formed, followed by a Cu_2O/Cu bulk layer between 530 and 600 K after the CuO phase was consumed. Above 600 K, we assumed a thin metallic copper layer on top of Cu_2O (i.e., a $Cu/Cu_2O/Cu$ bulk sequence). Above 670 K, the entire sample approached a pure metallic state. For the analysis, we do not explicitly consider a

Table 1
The optical constants n (refractive index), k (extinction coefficient) and φ_p (Brewster angle) for three different phases, Cu, Cu_2O, and CuO at a wavelength $\lambda = 6328$ Å [41]

Phase	n (refractive index)	k (extinction coefficient)	φ_p (Brewster angle)
Cu	0.237	−3.274	13.33°
Cu_2O	2.96	−0.12	71.33°
CuO	2.68	−0.45	69.50°

separate Cu_3O_2 layer, which is a defective Cu_2O phase, because the optical constants for this phase are not known [42–45].

The formulation of a $Cu_2O/CuO/Cu_2O/Cu$ bulk sequence in the range 490–520 K is consistent with previous results [15] and it is also in agreement with thermodynamics. The assumption of metallic Cu on top of Cu_2O at >600 K is supported by the XPS study of Poulston et al. [46] showing that vacuum annealing of Cu_2O at 770 K results in the formation of a thin metallic Cu film on top of Cu_2O.

The quality of the fit is demonstrated in Fig. 4, and the corresponding layer thicknesses are summarized in Table 2. The layer sequence, not the individual thickness values, should be considered the essential result of the fitting process. Precisely determining the layer thickness is difficult, however, for several reasons. The simulations, which are based on the Fresnel equations, assume strain-free and defect-free chemically homogeneous layers with sharp planar interfaces between them. This is clearly not the case here, as is evident from the images in Fig. 3 showing a strongly roughened surface. This roughening not only complicates the analysis, but also constitutes an experimental problem. Because the sample roughens dramatically during the reactions, subsequent realignment of the instrument is difficult, thus introducing an additional systematic error.

Keeping the limitations of the model in mind, the values listed in Table 2 describe the following process. As shown in Fig. 4, up to the ignition of the reaction, the Δ and Ψ values remain constant, corresponding to an approximately 1600-Å-thick CuO film on the copper substrate. At around 650 K, the Δ and Ψ values of metallic Cu are reached. Between 500 K and 520 K, the Δ and Ψ exhibit a pronounced dip and peak, respectively. To reproduce this dip/peak structure in the simulations, we had to assume a layer sequence consisting of a thin (only a

Table 2
Calculated layer sequences to simulate the observed values for Δ and Ψ of the experiment displayed in Fig. 4

T	Layer thicknesses	Simulation		Measurement	
		Δ	Ψ	Δ	Ψ
303 K	1600 Å CuO/Cu-bulk	25.73	15.70	25.64	19.56
403 K	1600 Å CuO/Cu-bulk	25.73	15.70	25.42	19.26
503 K	2 Å Cu_2O/1280 Å CuO/250 Å Cu_2O/Cu-bulk	25.64	21.45	25.74	21.39
518 K	5 Å Cu_2O/370 Å CuO/2200 Å Cu_2O/Cu-bulk	14.95	27.93	14.92	27.02
521 K	10 Å Cu_2O/220 Å CuO/2300 Å Cu_2O/Cu-bulk	26.06	30.52	26.15	30.46
533 K	3600 Å Cu_2O/Cu-bulk	40.37	27.02	40.03	22.30
573 K	3570 Å Cu_2O/Cu-bulk	48.47	26.53	48.39	22.88
603 K	10 Å Cu/3500 Å Cu_2O/Cu-bulk	76.03	26.35	75.95	27.00
623 K	20 Å Cu/2300 Å Cu_2O/Cu-bulk	95.33	32.31	95.68	29.93
653 K	50 Å Cu/1100 Å Cu_2O/Cu-bulk	108.9	38.72	108.9	32.74
723 K	Cu-bulk	105.8	43.16	112.5	37.07

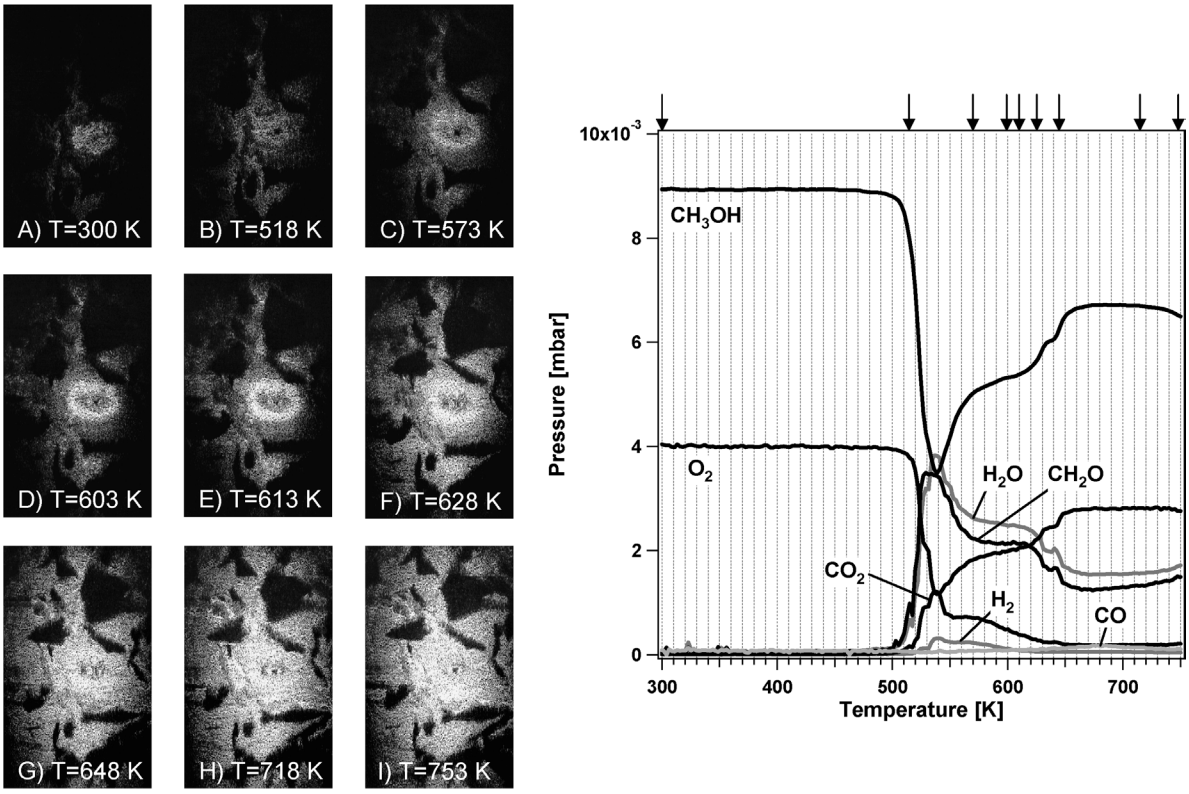

Fig. 5. Ellipsometric images during a TPR experiment over a deeply oxidized copper sample. Shown is the heating part of the experiment with a heating rate of 5 K/min. Left: an image series of a 1×1.8 mm^2 large sample area recorded with ellipsometric contrast; right: the corresponding TPR spectrum. The arrows above the panel indicate the reactivity corresponding to each image. Reaction conditions: CH_3OH flow rate 0.2 sccm and O_2 flow rate 0.1 sccm.

few Å) Cu_2O film on top of a relatively thick CuO layer separated from the metallic Cu substrate again by a Cu_2O layer. With progressive reduction, the CuO layer is transformed into Cu_2O, and finally a thick (several thousand Å) Cu_2O film remains on top of the metallic Cu substrate. This CuO reduction process is accompanied by a steep rise in reactivity. At the rate maximum at 540 K, a relatively thick Cu_2O film exists on the Cu surface. Both Δ and Ψ change very little in the subsequent T interval up to ≈570 K. Apparently, in this T window a stable and very reactive Cu_2O film exists on top of the metallic substrate.

We could model these changes in angles only by a decreasing Cu_2O thickness accompanied by the formation of a very thin (a few Å) metallic Cu film on top of the Cu_2O layer. Formation of the Cu film, terminating the sample surface, is associated with a decrease in reactivity of roughly 50%. As the Cu_2O layer is reduced, a rough metallic Cu substrate results, which flattens with progressive annealing until finally, at ≈720 K, a metallic shining Cu surface is created.

The changes in Δ and Ψ during the TPR experiment allow us to image the surface with ellipsometric contrast. In the microscope mode, the analyzer (A) and the polarizer (P) can be adjusted to nullsetting, so that only the intensity changes relative to this reference image are visible. Here nullsetting was done for the initial CuO phase. A significant problem arises from the surface roughening because the stray light is nonpolarized, and thus a relatively bright background signal exists that cannot be eliminated by nullsetting.

Surprisingly, even with such a rough surface, we could obtain images with ellipsometric contrast, as shown in Fig. 5, displaying images of the sample during a TPR experiment with a deeply oxidized copper surface. The experiment thus is very similar to that depicted in Fig. 3, but the contrast mechanism of the images is different and the images show a smaller section (only 1×1.8 mm^2) compared with the photographic images in Fig. 3, which show the complete sample (roughly 9×11 mm^2). Due to the grazing incidence of the laser beam, the images are focused precisely in only a narrow stripe perpendicular to the reflection plane. A completely focused image was constructed by putting together a set of nine images, in which the focus was shifted stepwise from the top to the bottom of the corresponding image.

The images show the reduction process as a brightening of the surface. The reduction starts in the center of the sample as a front-like propagation. Above 600 K, the area surrounding the reduced part becomes more or less spatially uniformly bright. The large dark areas that persist in the images originate from topographic contrast and represent shadows from protruding parts or deep troughs due to a macroscopic roughness of the surface.

Note that the reactivity peak at $T \approx 650$ K visible in Figs. 2 and 3 are absent in the TPR spectra of Figs. 4 and 5. This difference reflects the fact that it is difficult to reproduce a CuO film with exactly the same thickness in the preparation of the initial surface. The values of Δ and Ψ in Fig. 4 indicate that the sample at $T = 650$ K is already close to a completely re-

duced metallic state. The lower reactivity of the metallic state indicates that the most active state of the surface is not a completely reduced copper surface, but rather a surface that still contains some oxygen.

4. Discussion

4.1. Activity of oxide phases versus metallic copper

The initial motivation for this study was to conduct experiments in an intermediate pressure range between the atmospheric pressure and the low-pressure conditions of the UHV studies. The rise in pressure from the previously applied 10^{-5} to 10^{-2} mbar involved a strong modification of the original single crystal Cu(110) sample; consequently, oxide formation and a strong visible roughening of the surface occurred. Apparently, in the system investigated, the pressure gap problem cannot be really separated from the material gap problem, because a change in pressure automatically also modifies the substrate.

The kinetics that we measured here are qualitatively compatible with the low-pressure data obtained with the same Cu(110) sample [38,39]. According to the previous results, the low-temperature reactivity peak around 500 K should vanish beyond 10^{-3} mbar, and this was the case for the metallic copper surface, as shown in Fig. 2.

A surprising result of this study was the high reactivity of the oxidized surfaces. Over most of the T range, a high selectivity toward formaldehyde was maintained despite the availability of a large oxygen reservoir. This high reactivity of the oxidized samples does not contradict the results of Schlögl et al., who connected the active surface with a metallic state, because our experiments are transients, whereas in the steady-state conditions under which the near edge X-ray absorption fine structure (NEXAFS) and XPS experiments were carried out, the surface oxides would not persist [9–14,16].

Nevertheless, our experiments seem to indicate that oxide surfaces are more reactive than a metallic copper surface, as suggested by the correlation between the high rates and the visual impression of a colored surface (see Fig. 3). However, we must be aware that even if the first 10 or 100 layers of oxide were reduced to a metallic state before or during the ignition of the reaction, then the visual impression would still be that of an oxidized sample. Ellipsometry is in principle a surface-sensitive technique shown to be sensitive to adsorbates in the submonolayer range. But one must keep in mind that if the bulk properties were modified simultaneously, then the signal variations would be dominated by these latter changes, and, accordingly, surface modifications would be difficult to detect. The high reactivity seen in the black or red samples thus could be due to a partially reduced surface on top of a thick oxide layer. This would be in line with the general observation that perfect oxide surfaces are typically quite unreactive.

TPD experiments after methanol adsorption on Cu_2O and CuO powder samples gave a quite different product distribution than what we observed here [46]. Both oxide surfaces yielded CO_2 and H_2 as main products in the TPD experiments, a fact attributed to formation of formate as an intermediate species. Annealing the CuO powder at 800 K in vacuum produced a thick Cu_2O outermost layer. The reduction toward Cu_2O was prevented when the annealing was done in an oxygen atmosphere. On both CuO and Cu_2O/CuO surfaces, primarily total oxidation was observed in the TPD experiments, with the total oxidation more pronounced in the completely oxidized sample with a CuO surface. Annealing the Cu_2O powder sample in UHV at 770 K caused the formation of an outermost metallic Cu layer on top of Cu_2O [46]. Therefore, it is not surprising that such a sample exhibited nearly the same reactivity as metallic Cu surfaces in TPD experiments.

The thermal stability of the Cu oxides or Cu oxide films depends to some extent on their preparation, that is, oxide thickness, crystalline order, presence of impurities, and history [46–50]. The different preparation conditions mainly affect the kinetics of the reduction process. Similar, but less well-pronounced, effects have been reported for the oxidation kinetics [51].

In particular, Lee et al. [47] reported that for fully oxidized Cu films, CuO starts to decompose into Cu_2O during annealing in vacuum at 473 K, in accordance with measurements on CuO powder samples [49]. This temperature is very similar to the measured ignition temperature of the reaction in our experiments. In contrast, in another study [48], the transformation of CuO into Cu_2O was found to start at a considerably higher temperature (573 K). The $CuO \rightarrow Cu_2O$ transition appears to be completed at 573–673 K [47,49]. The subsequent vacuum decomposition of Cu_2O to metallic copper does not start below $T = 573$ K [48]; onset temperatures for this process are between 673 and 700 K [47,49].

The decomposition temperatures have been shown to be very different on a partially oxidized Cu film, where no traces of CuO were found above 380 K. The complete reduction of Cu_2O to metallic copper was already completed above 573 K [47].

The decomposition of CuO can occur via the reaction $CuO + Cu \rightarrow Cu_2O$. This reaction is exergonic at 298 K [47] and becomes more exergonic at elevated temperatures, whereas the decomposition of CuO via the thermal desorption of O_2 according to $CuO \rightarrow Cu + \frac{1}{2}O_2$ is highly endergonic and requires temperatures beyond the range of our experiments. In contrast, the reduction of CuO with methanol is highly exergonic (for oxygen being not too excessive in methanol/oxygen mixtures). Therefore, under our reaction conditions, the surface of CuO will be reduced quite rapidly by methanol, whereas the foregoing synproportionation to Cu_2O will take place at the CuO/Cu bulk interface. The CuO phase will thus be sandwiched between two Cu_2O layers of different thickness, as was determined experimentally in the temperature range 500–530 K.

4.2. The role of subsurface oxygen

Recent in situ NEXAFS spectroscopy and XPS experiments with polycrystalline Cu samples in the mbar range demonstrated that the surface of the copper catalyst is metallic in its active state [9–14,16]. However, the same NEXAFS study detected a new suboxide species in reaction conditions. NEXAFS

probes the outermost ∼500 Å of a solid and thus in principle provides a bulk characterization. To be surface sensitive, in situ high-pressure (mbar range) XPS was applied. With this technique, new oxygen adsorption states were identified and assigned to oxygen located in the subsurface region [13,14,16].

A point that should be considered more closely is the assignment of the O 1*s* state at 530.4 eV to subsurface oxygen [16]. Oxygen in Cu_2O has the same binding energy, but based on the fact that the copper surface is still metallic and due to the photon variation experiments, this state was assigned to subsurface oxygen. In the light of the finding of Poultson et al. that a thin metallic Cu layer sits on top of Cu_2O after annealing beyond 770 K in vacuum, a more heterogeneous surface composition also should be considered. Moreover, a spatially nonuniform surface, consisting of metallic Cu and Cu_2O, also perhaps should be taken into account. Irrespective of the exact identification of the O state at 530.4 eV reported earlier [16], a suboxide species seems to be necessary to optimize the catalytic activity of the copper surface.

Our measurements are not sensitive enough to confirm or reject the participation of subsurface oxygen in the reaction. However, if such a species exists, it should form at the metal/oxide interfaces of the oxidized samples as a precursor to the chemical transformations that occur in our system. The high reactivity that we observe might be due at least partially to the presence of this species. Clearly, further in situ studies with surface-sensitive techniques are needed to clarify this point.

4.3. Morphological changes

Quite generally, surfaces are modified by a catalytic reaction, with the extent depending on the reaction conditions and the reaction system. As shown in Fig. 3, the case of selective methanol oxidation demonstrates a quite dramatic effect. The oxidation of an originally flat surface causes a visible roughening on a ≈100-μm scale as CuO is formed, but the surface becomes flat again as the sample is reduced by methanol. Oxide formation on copper surfaces in a tarnishing process is a classical problem in solid-state chemistry. The basic problem to be solved is that of the mass transport of oxygen and copper, as outlined in some paradigmatic papers by Wagner [52,53]. On a microscale, stepped Cu surfaces have been shown to undergo faceting during exposure to oxygen [54].

The role of oxides in methanol oxidation over copper has been discussed not only because of their potential contribution to the overall activity, but also because the oxide/Cu interface has been made responsible for the strain in the metallic phase, which supposedly enhances the catalytic activity [55]. The mass transport of Cu that occurs as the copper oxide is reduced might generate unstable and reactive configurations, and if stress relief is not fast enough, strain will build up, leading to a catalyst with a different reactivity, as shown in recent quantum chemical calculations [56,57]. It can be speculated that this mass transport of Cu is responsible for the reactivity peak slightly above 500 K shown in Fig. 3. Because a restructuring of the Cu surface will facilitate penetration of oxygen into the Cu bulk region, the formation of subsurface oxygen is probably intertwined with the morphological changes induced by the reaction on the catalytic surface. Both processes are favored by oxide formation, so that ultimately various properties are probably more or less inseparably connected.

5. Conclusions

We compared the reactivity of a metallic Cu sample with strongly oxidized Cu samples in the 10^{-2} mbar range using in situ ellipsometry to monitor changes in the chemical composition in the near surface region. The kinetics that we measured in the TPR experiments are transients, because the oxidized surface is reduced during the TPR experiment, finally resulting in a metallic surface. Our main observations and results can be summarized as follows:

1. The reactivity of the oxidized surfaces is higher than that of a metallic copper surface, whereas the fairly high selectivity to formaldehyde is maintained over most of the parameter range. We conclude that the chemical change from CuO over Cu_2O to metallic Cu has a strong beneficial effect on the reactivity of the sample.
2. A direct indication of what might stimulate the reactivity of the surface is given by photographic images demonstrating a dramatic roughening/flattening of the surface during the TPR experiment. Apparently, the restructuring of the surface during oxidation/reduction creates very reactive surface configurations that appear as transients of high reactivity in the rate measurements.
3. The ellipsometric data demonstrate that the reduction of the oxidized surfaces proceeds through sandwich structures in the chemical composition in which initially CuO and later Cu_2O are sandwiched between more reduced phases, one forming the interface to the Cu bulk and the other representing the surface layer. Accordingly, at around 500 K, CuO is sandwiched between two Cu_2O layers, and at around 600 K, a Cu_2O phase is sandwiched between metallic Cu on both sides.

Clearly, a detailed microscopic picture of the atomic configurations responsible for the high reactivity cannot be given on the basis of our data; that is, whether it is strain or subsurface oxygen or a combination of both is not clear. This requires further in situ studies with suitable surface analytical tools. What the data do convincingly demonstrate, however, is that the dynamics of the reaction system are quite high at 10^{-2} mbar and that the high reactivity that we observe is probably caused largely by these dynamic changes in surface chemical composition and morphology.

Acknowledgment

This work was supported by the DFG through the priority program 1091, “Bridging the Gap Between Ideal and Real Systems in Heterogeneous Catalysis.”

References

[1] C.N. Satterfield, Heterogeneous Catalysis in Practice, McGraw-Hill, New York, 1980.
[2] C.L. Thomas, Catalytic Processes and Proven Catalysts, Academic Press, New York, 1970.
[3] J. Walker, Formaldehyde, Reinhold, Amsterdam, 1964.
[4] Ullmann, Encyclopedia of Industrial Chemistry, Verlag Chemie, Weinheim, 1982.
[5] E. Jones, G. Fowlie, J. Appl. Chem. 3 (1953) 206.
[6] P.L. Hansen, J.B. Wagner, S. Helveg, J.R. Rostrup-Nielsen, B.S. Clausen, H. Topsoe, Science 295 (2002) 2053.
[7] M.M. Günter, T. Ressler, B. Bems, C. Büscher, T. Genger, O. Hinrichsen, M. Muhler, R. Schlögl, Catal. Lett. 71 (2001) 37.
[8] H. Werner, D. Herein, G. Schulz, U. Wild, R. Schlögl, Catal. Lett. 49 (1997) 109.
[9] A. Knop-Gericke, M. Hävecker, T. Schedel-Niedrig, R. Schlögl, Top. Catal. 10 (2000) 187.
[10] A. Knop-Gericke, M. Hävecker, T. Schedel-Niedrig, R. Schlögl, Top. Catal. 15 (1) (2001) 27.
[11] T. Schedel-Niedrig, T. Neisius, I. Böttger, E. Kitzelmann, G. Weinberg, D. Demuth, R. Schlögl, Phys. Chem. Chem. Phys. 2 (2000) 2407.
[12] I. Böttger, T. Schedel-Niedrig, O. Timpe, R. Gottschall, M. Hävecker, T. Ressler, R. Schlögl, Chem. Eur. J. 6 (2000) 1870.
[13] V.I. Bukhtiyarov, I.P. Prosvirin, E.P. Tikhomirov, V.V. Kaichev, A.M. Sorokin, V.V. Evstigneev, React. Kinet. Catal. Lett. 79 (2003) 181.
[14] I.P. Prosvirin, E.P. Tikhomirov, A.M. Sorokin, V.V. Kaichev, V.I. Bukhtiyarov, Kinet. Catal. 44 (2003) 662.
[15] A. Kudelski, B. Pettinger, Surf. Sci. 566–568 (2004) 1007.
[16] H. Bluhm, M. Hävecker, A. Knop-Gericke, E. Kleimenov, R. Schlögl, D. Teschner, V.I. Bukhtiyarov, D.F. Ogletree, M. Salmeron, J. Phys. Chem. B 108 (2004) 14340.
[17] I.E. Wachs, R.J. Madix, J. Catal. 53 (1978) 208.
[18] M. Bowker, R.J. Madix, Surf. Sci. 95 (1980) 190.
[19] A.F. Carley, A.W. Owens, M.K. Rajumon, M.W. Roberts, Catal. Lett. 37 (1996) 79.
[20] S.M. Francis, F.M. Leibsle, S. Haq, N. Xiang, M. Bowker, Surf. Sci. 315 (1994) 284.
[21] F.M. Leibsle, S.M. Francis, S. Haq, M. Bowker, Surf. Sci. 318 (1994) 46.
[22] S.L. Silva, R.M. Lemor, F.M. Leibsle, Surf. Sci. 421 (1999) 135.
[23] S.L. Silva, R.M. Lemor, F.M. Leibsle, Surf. Sci. 421 (1999) 146.
[24] A.F. Carley, P.R. Davies, G.G. Mariotti, S. Read, Surf. Sci. 364 (1996) 525.
[25] M. Bowker, Top. Catal. 3 (1996) 461.
[26] P.R. Davies, G.G. Mariotti, J. Phys. Chem. 100 (1996) 19975.
[27] R.J. Madix, S.G. Telford, Surf. Sci. 328 (1995) 576.
[28] J. Nakamura, Y. Kushida, Y. Choi, T. Uchijima, T. Fujitani, J. Vac. Sci. Technol. A 15 (1997) 1568.
[29] Z.-M. Hu, K. Takahashi, H. Nakatsuji, Surf. Sci. 442 (1999) 90.
[30] A. Sotiropoulos, P.K. Milligan, B.C.C. Cowie, M. Kadodwala, Surf. Sci. 444 (2000) 52.
[31] M.A. Karolewski, R.G. Cavell, Appl. Surf. Sci. 173 (2001) 151.
[32] K. Mudalige, M. Trenary, Surf. Sci. 504 (2002) 208.
[33] F.M. Leibsle, Surf. Sci. 401 (1998) 153.
[34] P.R. Davies, G.G. Mariotti, Catal. Lett. 43 (1997) 261.
[35] A.H. Jones, S. Poulston, R.A. Bennett, M. Bowker, Surf. Sci. 380 (1997) 31.
[36] B.A. Sexton, A.E. Hughes, N.R. Avery, Surf. Sci. 155 (1985) 366.
[37] J.N. Russell, S.M. Gates, J.T. Yates, Surf. Sci. 163 (1985) 516.
[38] L. Zhou, S. Günther, R. Imbihl, J. Catal. 230 (2005) 166.
[39] L. Zhou, S. Günther, R. Imbihl, J. Catal. 232 (2005) 295.
[40] M. Harke, R. Teppner, O. Schulz, H. Motschmann, H. Orendi, Rev. Sci. Instrum. 68 (1997) 3130.
[41] E.D. Palik, Handbook of Optical Constants of Solids, Academic Press, Boston, 1985.
[42] D.L. Cocke, D.E. Mencer, M.A. Hossain, R. Schennach, M. Kesmez, J.R. Parge, D.G. Naugle, J. Appl. Electrochem. 34 (2004) 919.
[43] D.E. Mencer, M.A. Hossain, R. Schennach, T. Grady, H. McWhinney, J.A.G. Gomes, M. Kesmez, J.R. Parga, T.L. Barr, D.L. Cocke, Vacuum 77 (2004) 27.
[44] R. Schennach, A. Gupper, Mat. Res. Soc. Symp. Proc. 766 (2003) E3.2.1.
[45] D.L. Cocke, R. Schennach, M.A. Hossain, D.E. Mencer, H. McWhinney, J.R. Pargae, M. Kesmez, J.A.G. Gomes, M.Y.A. Mollah, Vacuum 79 (2005) 71.
[46] S. Poulston, E. Rowbotham, P. Stone, P. Parlett, M. Bowker, Catal. Lett. 52 (1998) 63.
[47] S.Y. Lee, N. Mettlach, N. Nguyen, Y.M. Sun, J.M. White, Appl. Surf. Sci. 206 (2003) 102.
[48] J. Li, G. Vizkelethy, P. Revesy, J.W. Mayer, L.J. Matienzo, F. Emmi, C. Ortega, J. Siejka, Appl. Phys. Lett. 58 (1991) 1344.
[49] S. Poulston, P.M. Parlett, M. Bowker, Surf. Interface Anal. 24 (1996) 811.
[50] P.D. Kirsch, J.G. Ekerdt, J. Appl. Phys. 90 (2001) 4256.
[51] M. Rauh, P. Wißmann, Thin Solid Films 228 (1993) 121.
[52] C. Wagner, K. Grünewald, Z. Phys. Chem. B 40 (1938) 455.
[53] H. Schmalzried, Solid State Reactions, Verlag Chemie & Academic Press, Weinheim, 1974.
[54] N. Reinecke, S. Reiter, S. Vetter, E. Taglauer, Appl. Phys. A 75 (2002) 1.
[55] F. Girgsdies, T. Ressler, U. Wild, T. Wübben, T.J. Balk, G. Dehm, L. Zhou, S. Günther, E. Arzt, R. Imbihl, R. Schlögl, Catal. Lett. 102 (2005) 91.
[56] S. Sakong, A. Gross, J. Catal. 231 (2005) 420.
[57] Y. Xu, M. Mavrikakis, Surf. Sci. 494 (2001) 131.